Supplement to: Which multiband factor should you choose for your resting-state fMRI study?

Benjamin B. Risk[a,*], Raphiel J. Murden[a], Junjie Wu[b], Mary Beth Nebel[c,d], Arun Venkataraman[e], Zhengwu Zhang[f], Deqiang Qiu[b]

[a]*Department of Biostatistics and Bioinformatics, Emory University*
[b]*Department of Radiology and Imaging Sciences*
[c]*Center for Neurodevelopmental and Imaging Research, Kennedy Krieger Institute*
[d]*Department of Neurology, Johns Hopkins University School of Medicine*
[e]*Department of Physics and Astronomy, University of Rochester, Rochester, NY, United States*
[f]*Department of Statistics and Operations Research, University of North Carolina at Chapel Hill, USA*

S.1. Supplemental Materials for Results: Noise amplification

[*]1518 Clifton Rd NE, Atlanta, GA 30322
*Email address:* benjamin.risk@emory.edu (Benjamin B. Risk)
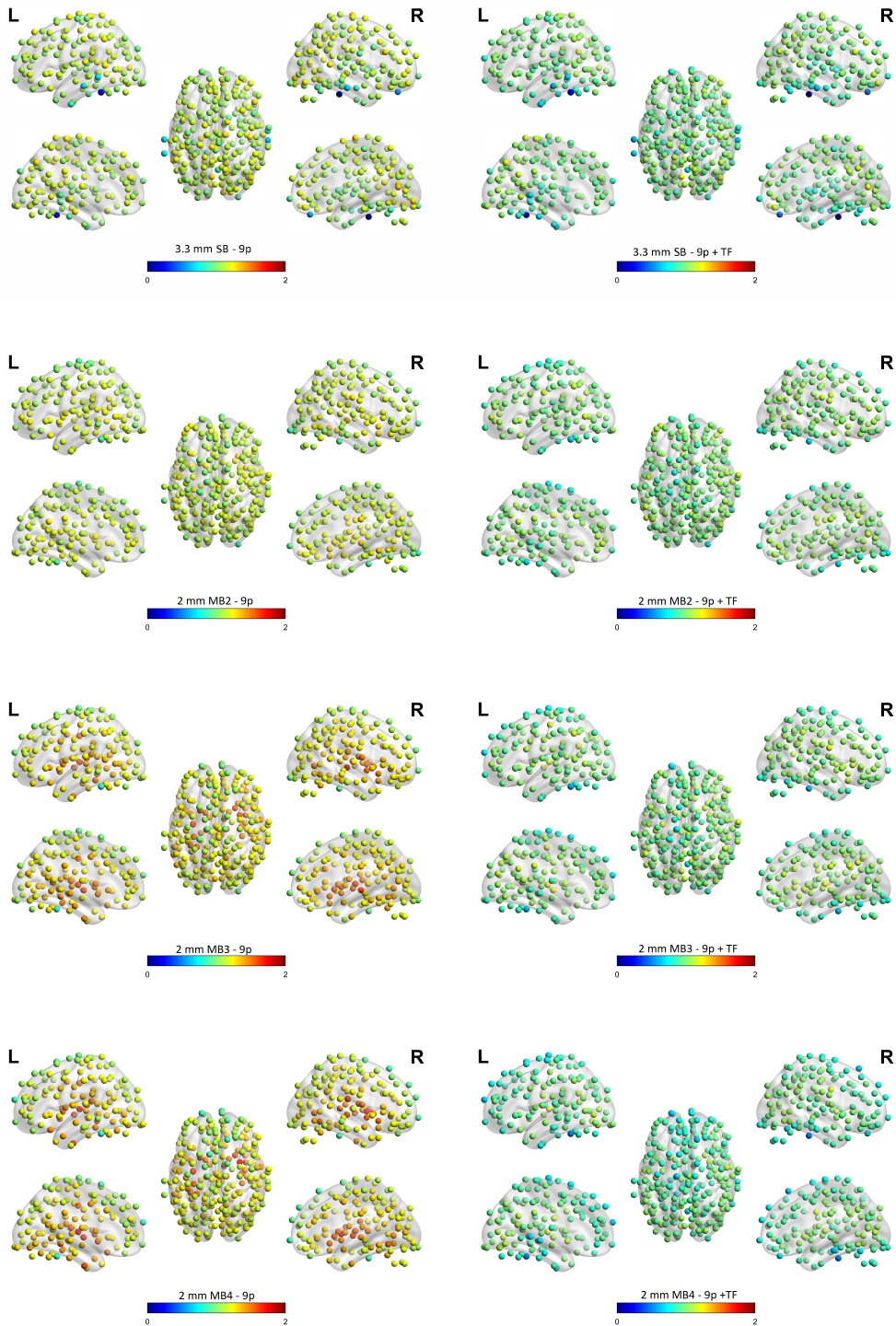
Figure S.1: Brain net visualization of noise amplification in the Power-264 atlas. Nodes are colored according to their noise amplification, where the noise amplification is based on the median apparent g-factor across thirty-two subjects. This figure contains the apparent g-factors for the single-band 3.3 mm (relative to single-band 2 mm), MB 2, MB 3, and MB 4. Left-side: 9p preprocessing. Right-side: 9p+bandpass.
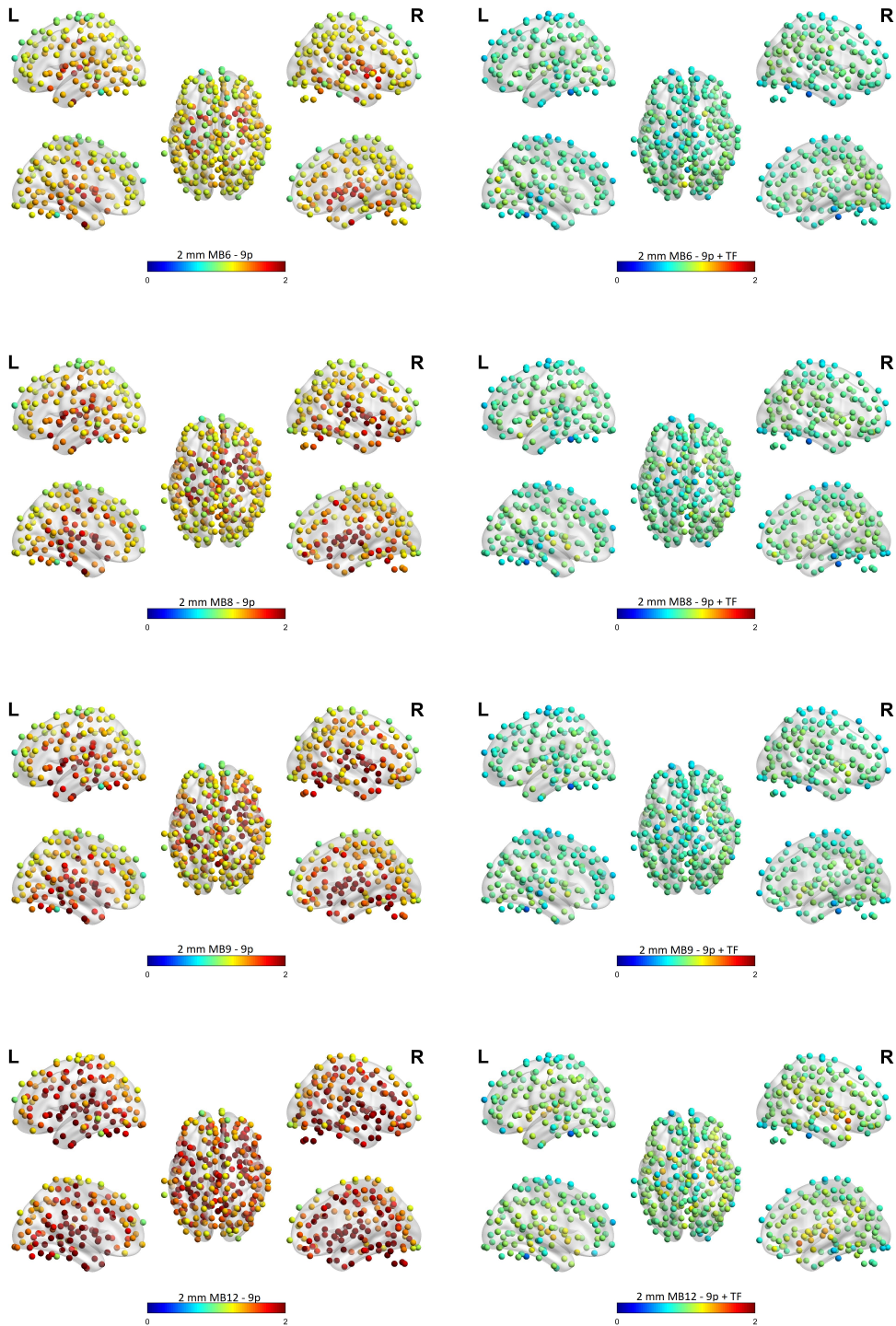
Figure S.2: Brain net visualization of noise amplification in the Power-264 atlas. Nodes are colored according to their noise amplification, where the noise amplification is based on the median apparent g-factor across thirty-two subjects. This figure contains the apparent g-factors for the MB 6 (relative to single-band 2 mm), MB 8, MB 9, and MB 12. Left-side: 9p preprocessing. Right-side: 9p+bandpass.

3
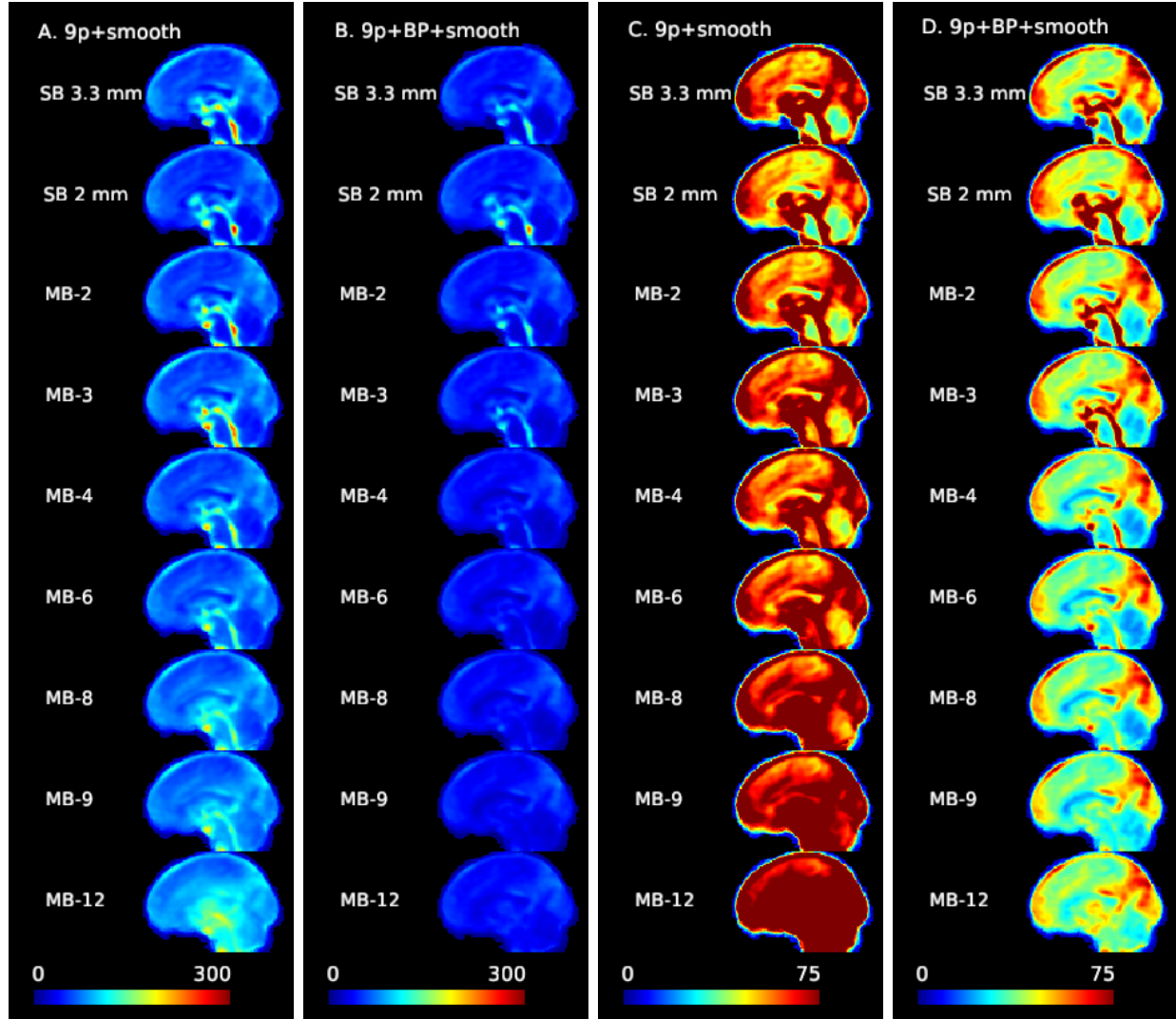
Figure S.3: Noise amplification due to multiband acceleration and impacts of bandpass filtering in spatially smoothed data (6-mm FWHM Gaussian kernel). The standard deviation of the time series for each voxel (averaged across subjects) with 9p preprocessing (columns 1 and 3) and 9p+bandpass (columns 2 and 4). Sagittal slice with cursor at MNI=0. At higher MB factors, variance from noise amplification becomes more prominent. Columns 1 and 2 use a scale from 0 to 300, and columns 3 and 4 are the same data but scaled from 0 to 75. Relative to unsmoothed data (Figure 1 of the main manuscript), the standard deviation is greatly reduced, as expected. However, the noise amplification increases with MB factor in the 9p+smooth pipeline (column C), similar to the unsmoothed data.

S.2. Supplemental Materials for Results: Impacts on seed map correlations
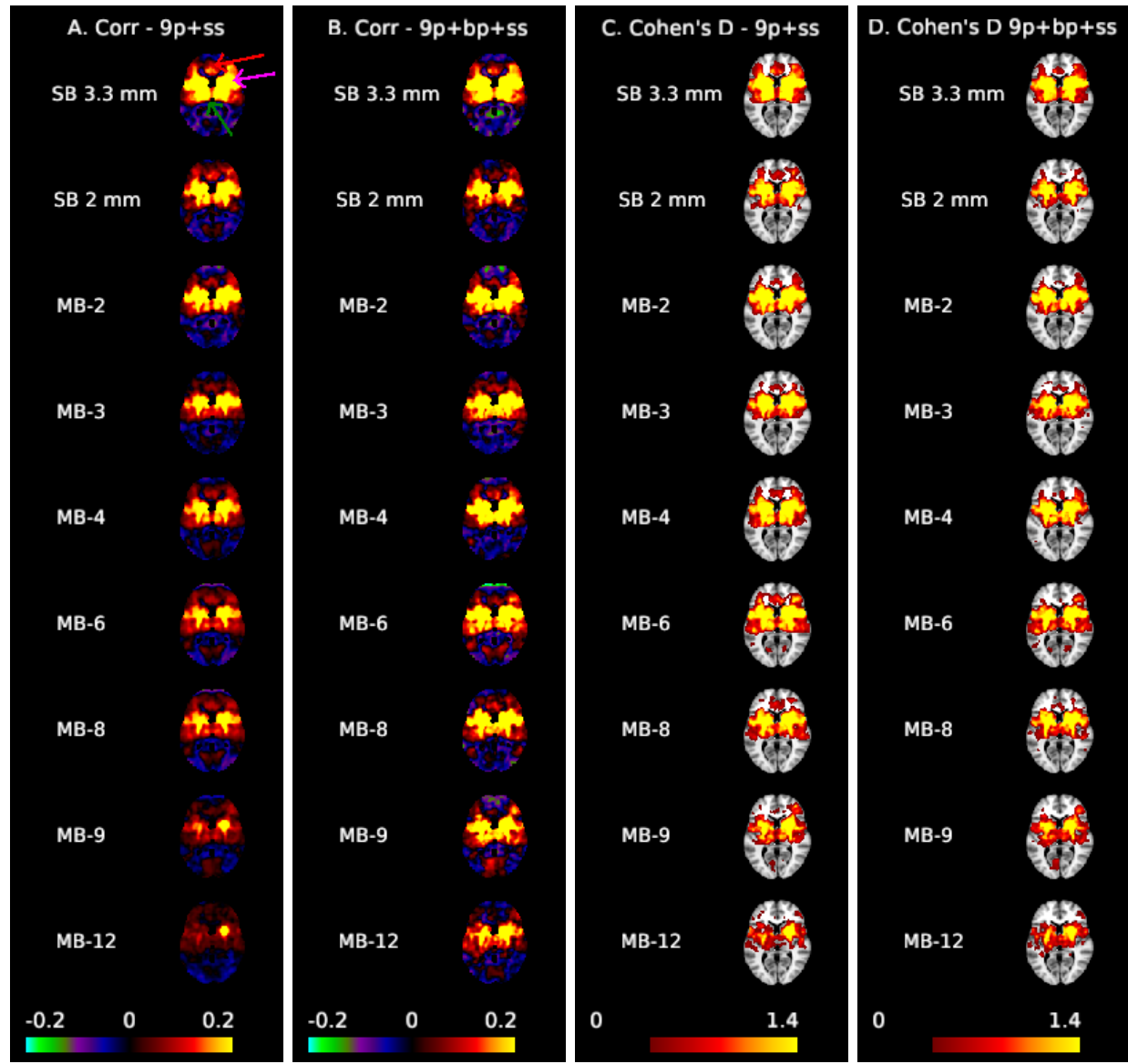
Figure S.4: Correlation (A,B) and Cohen's d maps (C,D, thresholded to display values >0.4) for the dorsal rostral putamen seed (MNI: 25, 8, 6) in spatially smoothed data (6-mm FWHM) shown at MNI axial slice 6. The arrows in Figure A highlight the cingulate cortex (red), insula (fuchsia), and thalamus (green). The color gradient used in this image is identical to Figure 2 of the main manuscript. Relative to preprocessing without spatial smoothing, spatial smoothing increases effect sizes, including in many white matter regions. This leads to an increase in sensitivity but a decrease in specificity, as large effect sizes extend to white matter areas and across contiguous regions merging the insula and putamen. Effect sizes are largest in SB 3.3 mm.
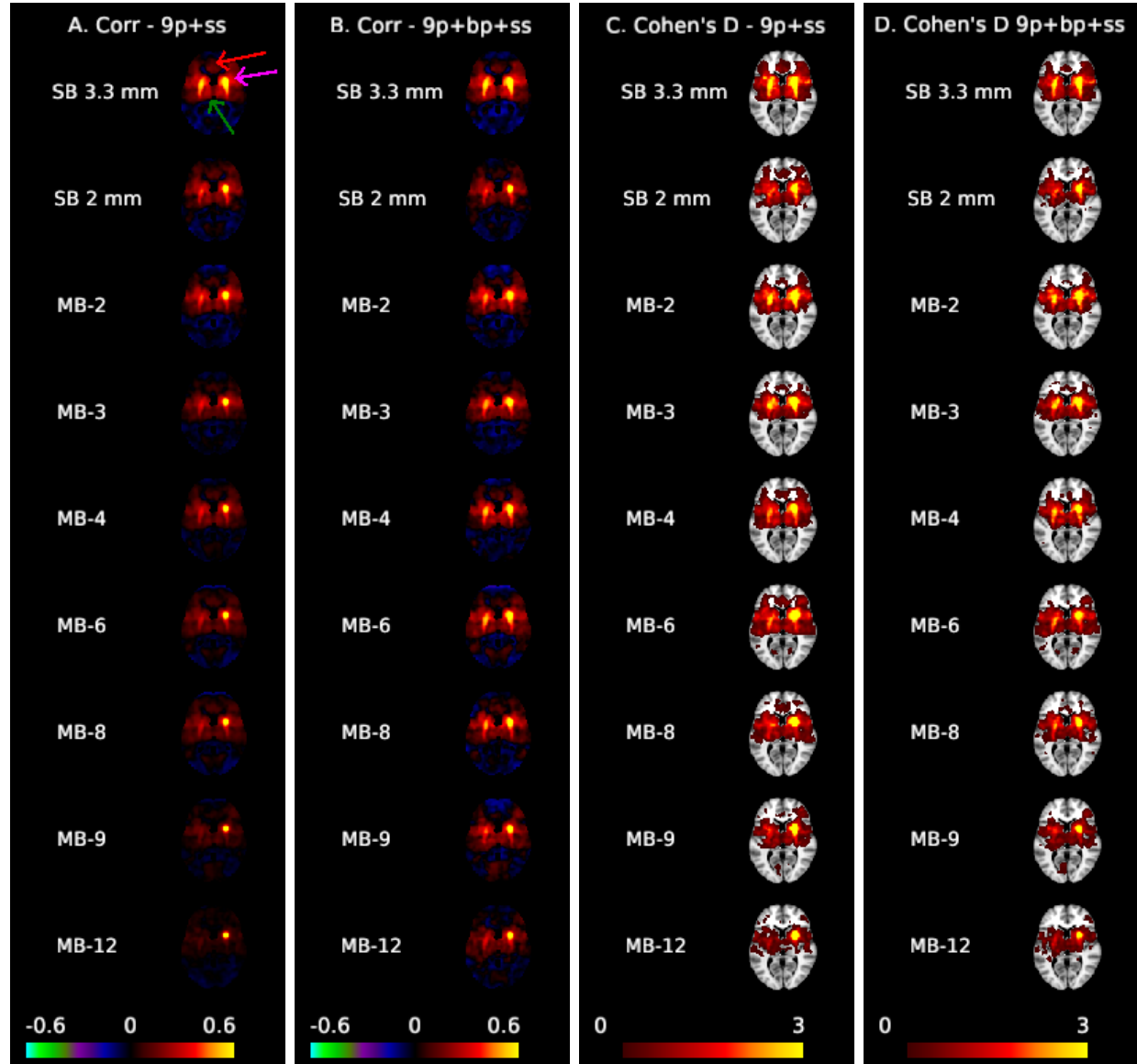
Figure S.5: Correlation (A,B) and Cohen's d maps (C,D, (thresholded to display values >0.4) for the dorsal rostral putamen seed (MNI: 25, 8, 6) in spatially smoothed data (6-mm FWHM) shown at MNI axial slice 6. This figure is identical to Figure S.4 except the color gradients have been changed to increase the contrast. As in the 9p and 9p+bp without spatial smoothing, SB 3.3 mm captures putamen functional connectivity better than the 2 mm and multiband acquisitions.
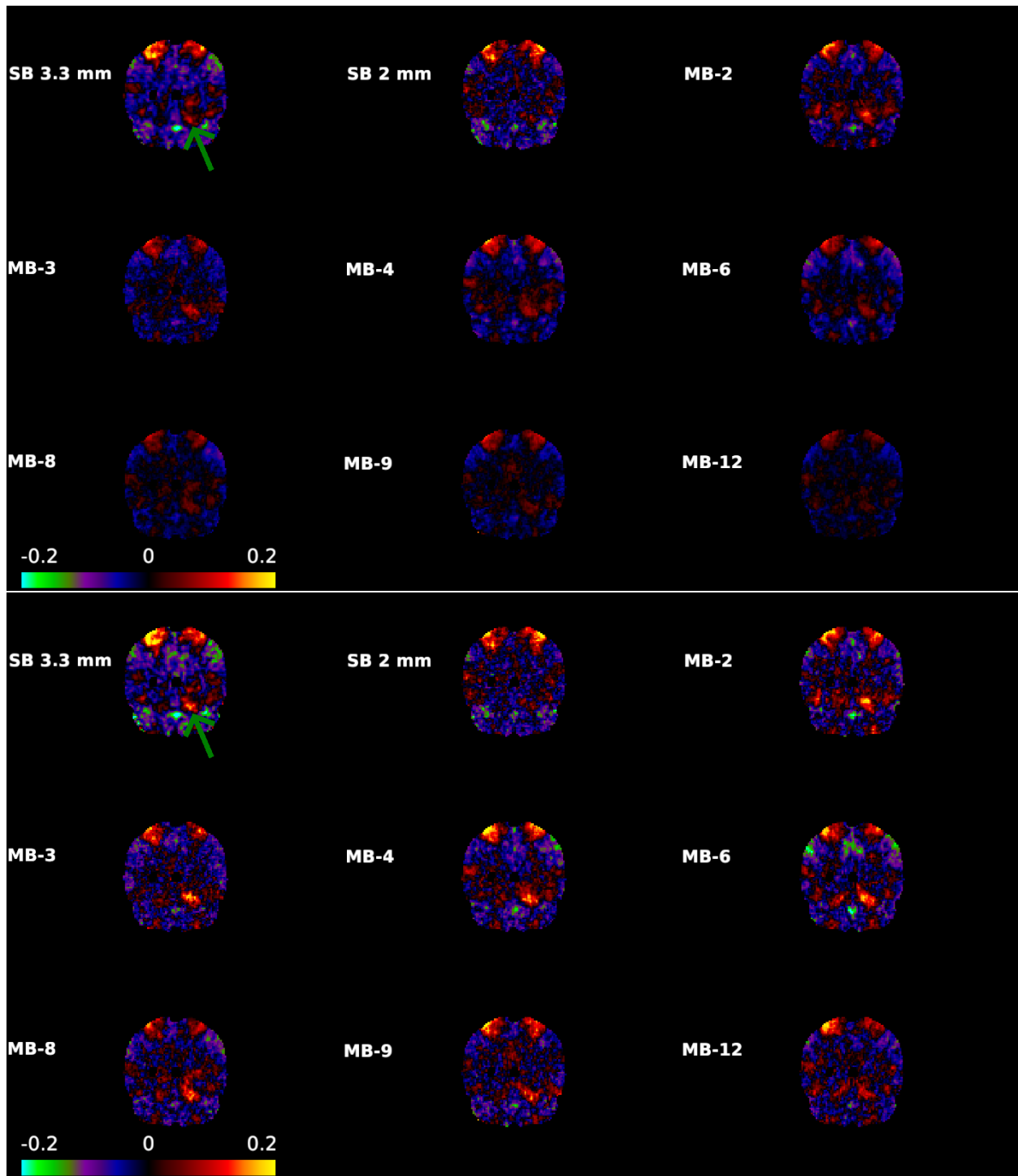
Figure S.6: Correlation maps at MNI coronal slice -55 for the motor seed (-41, -20, 62). The green arrow points to an area in the right cerebellum that was correlated with the left motor cortex in Buckner et al. (2011). This area is only faintly apparent in most acquisitions in 9p (top), with largest correlations at MB 2 (around 0.10), most acquisitions around 0.05, and small or negligible correlations in SB 2 mm and MB 12. The region is more apparent in 9p+bandpass (bottom), with correlations greater than 0.10 for SB 3.3, MB 2, 3, 4, 6, 8, and 9, but are poorly captured at SB 2 mm and MB 12.
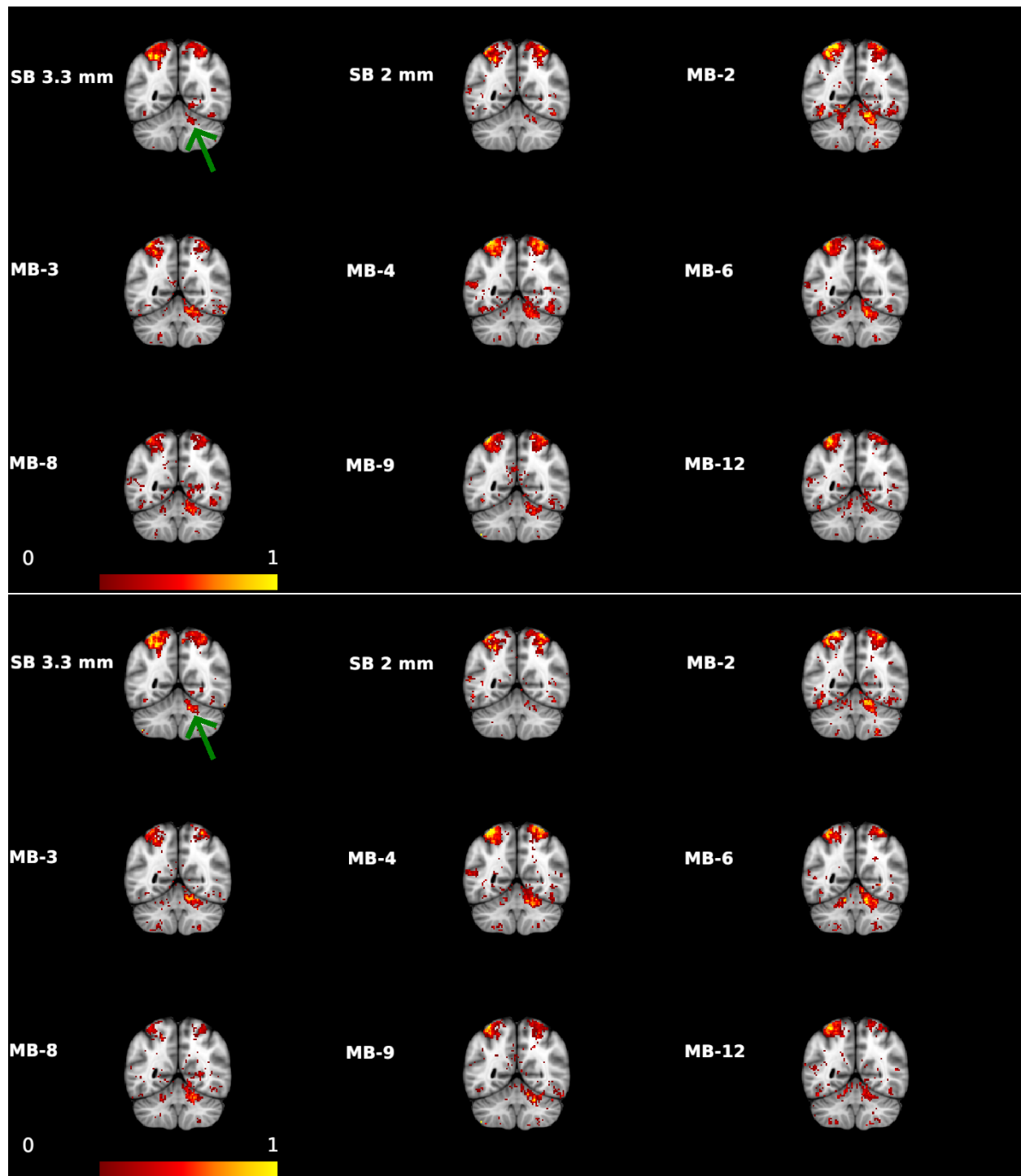
Figure S.7: Cohen's d maps at MNI coronal slice -55 for the motor seed (-41, -20, 62). The green arrow points to an area in the right cerebellum that was correlated with the left motor cortex in Buckner et al. (2011). The area is best represented by MB 2 in both 9p (top) and 9p+bandpass (bottom), with comparable spatial extents from MB 2 to MB 8.

S.3. Supplemental Materials for Results: Impacts on pairwise correlations in a functional atlas
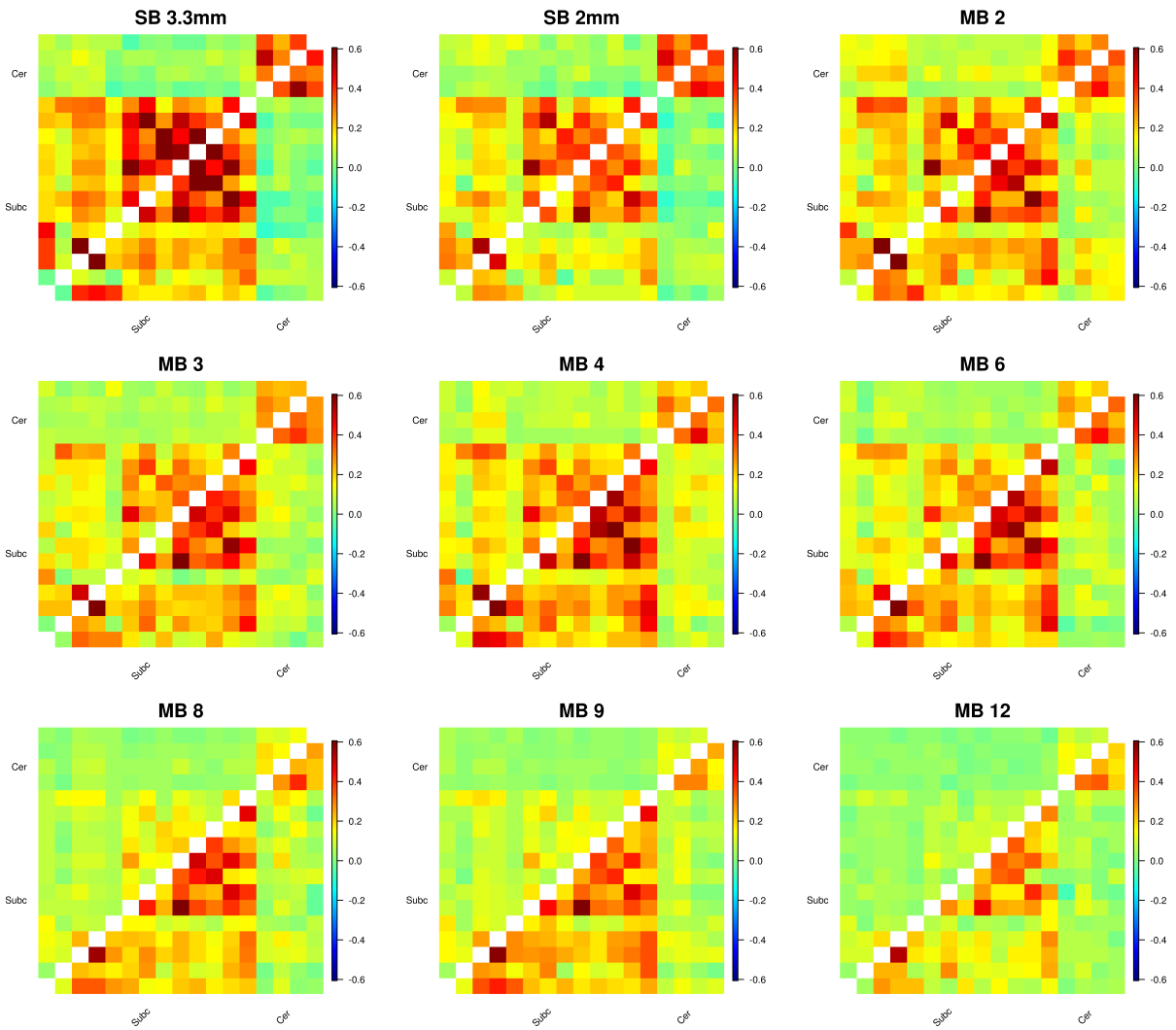
Figure S.8: Average correlation (Fisher z-transformed) for SB and MB acquisitions in subcortical and cerebellar regions. Correlations without temporal filtering are above the diagonal and correlations with bandpass filtering are below the diagonal.
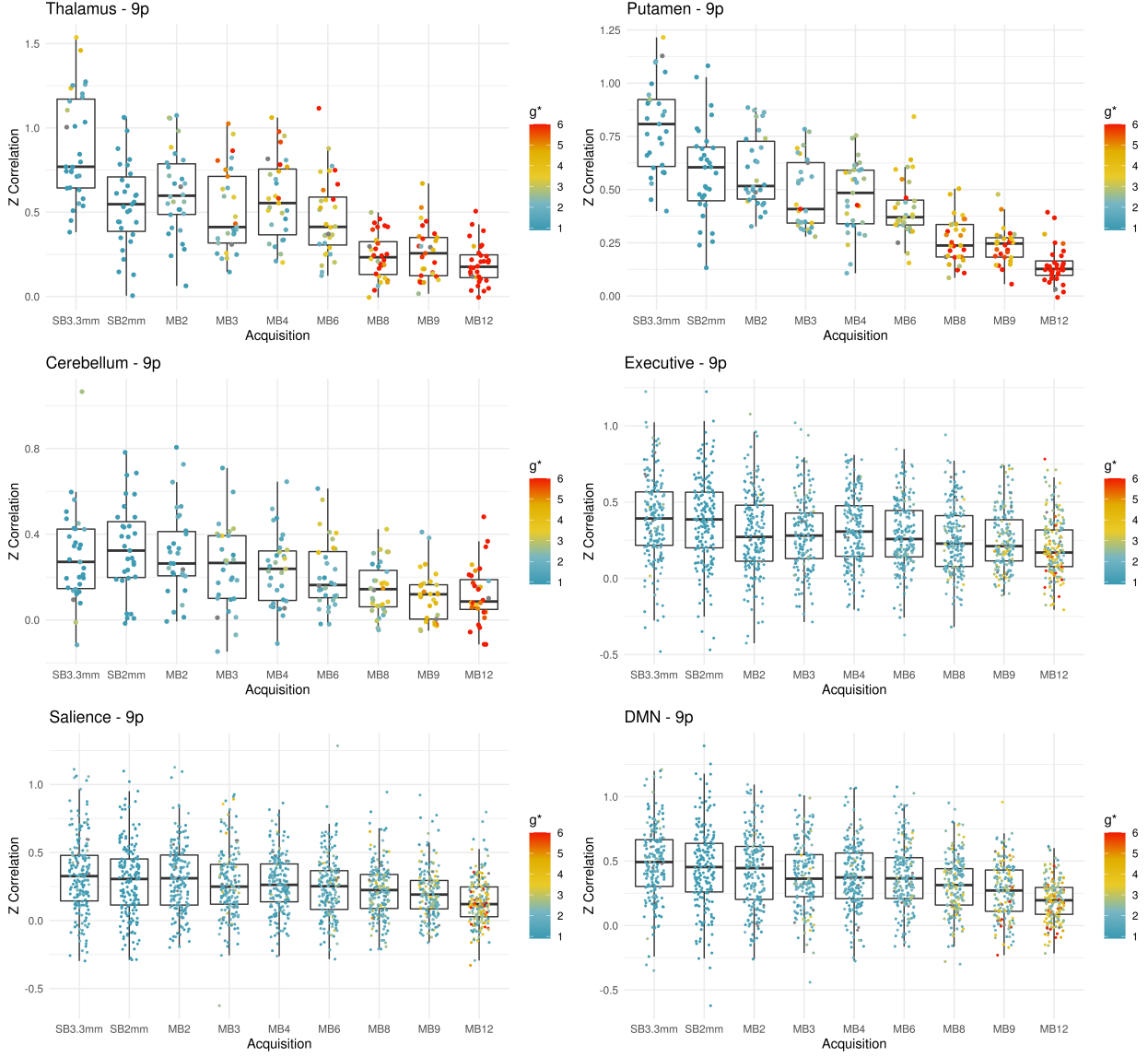
Figure S.9: The impact of multiband acquisition on within community Fisher z-transformed correlations in the 9p pipeline. Each data point is the correlation between nodes for a participant in the indicated community and acquisition. Thalamus, putamen, and cerebellum based on two nodes each, and executive control, salience, and default mode network based on four nodes each (6 correlations / participant). The points are colored according to the participant-specific $g*$-factor.
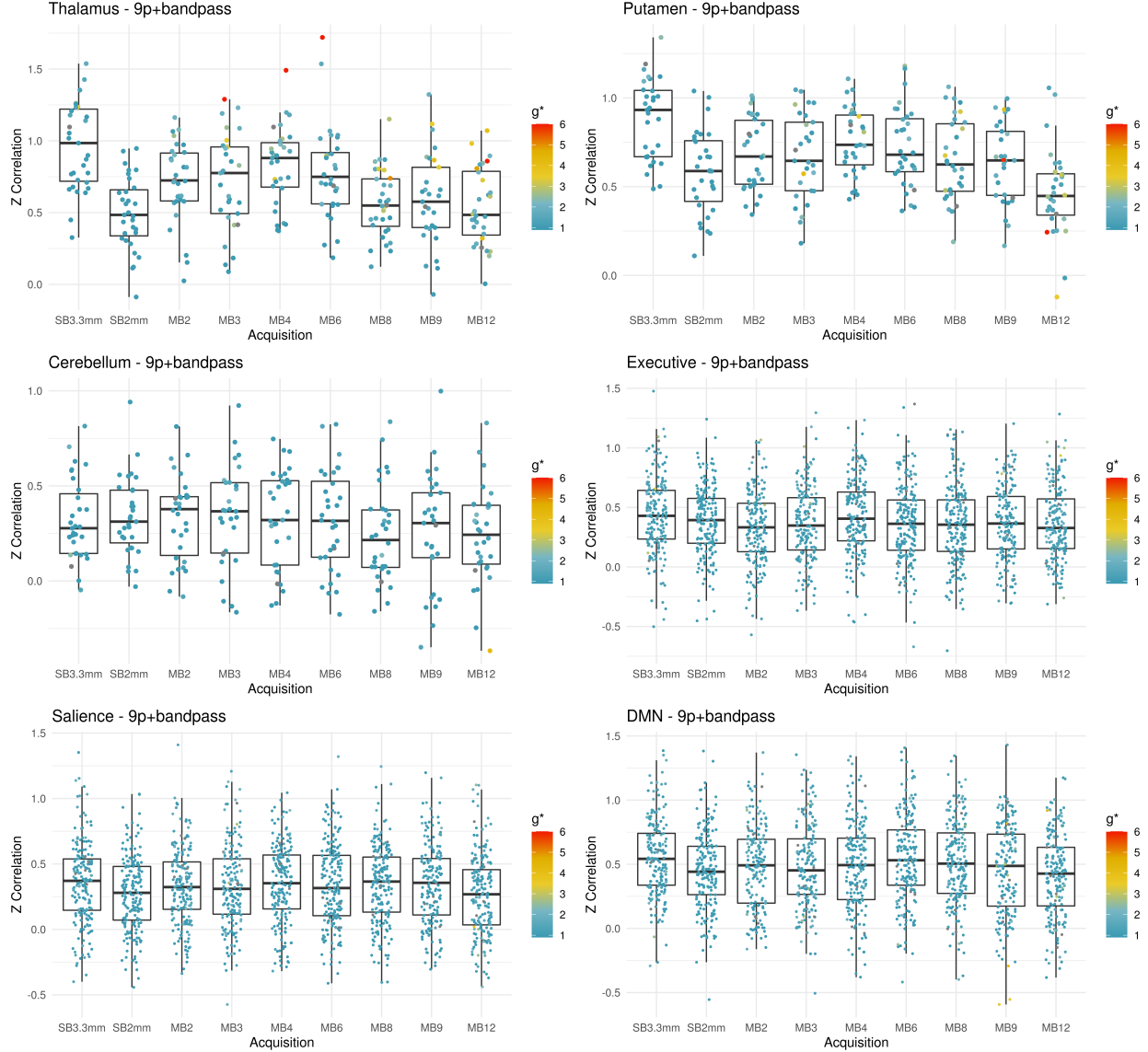
Figure S.10: The impact of multiband acquisition on within community Fisher z-transformed correlations in the 9p+bandpass pipeline. Each data point is the correlation between nodes for a participant in the indicated community and acquisition. Thalamus, putamen, and cerebellum based on two nodes each, and executive control, salience, and default mode network based on four nodes each (6 correlations / participant). The points are colored according to the participant-specific $g*$-factor.

|	Thal 9p+ss	Puta 9p+ss	Cere 9p+ss	Exec 9p+ss	Sali 9p+ss	DMN 9p+ss
Int.	0.7(0.06)	0.77(0.05)	0.39(0.04)	0.49(0.03)	0.36(0.04)	0.55(0.04)
SB3.3	**0.34(0.08) <.001**	**0.22(0.05) <.001**	-0.06(0.04) 0.189	-0.01(0.03) 0.854	0.04(0.03) 0.145	0.06(0.05) 0.186
MB 2	0.06(0.06) 0.268	-0.02(0.04) 0.652	-0.06(0.04) 0.214	**-0.12(0.04) 0.002**	0(0.04) 0.9	0(0.03) 0.989
MB 3	-0.04(0.06) 0.508	**-0.1(0.04) 0.006**	-0.1(0.05) 0.037	**-0.09(0.03) 0.006**	-0.04(0.03) 0.241	-0.04(0.03) 0.205
MB 4	0.02(0.06) 0.763	**-0.12(0.04) 0.002**	**-0.11(0.04) 0.004**	-0.07(0.04) 0.064	-0.03(0.03) 0.291	-0.06(0.03) 0.048
MB 6	-0.11(0.06) 0.067	**-0.21(0.04) <.001**	**-0.14(0.04) 0.001**	**-0.1(0.03) 0.002**	-0.06(0.03) 0.036	-0.05(0.04) 0.139
MB 8	**-0.38(0.06) <.001**	**-0.38(0.04) <.001**	**-0.22(0.03) <.001**	**-0.13(0.03) <.001**	**-0.09(0.02) <.001**	**-0.12(0.03) <.001**
MB 9	**-0.36(0.06) <.001**	**-0.41(0.04) <.001**	**-0.27(0.03) <.001**	**-0.14(0.03) <.001**	**-0.12(0.02) <.001**	**-0.16(0.03) <.001**
MB 12	**-0.44(0.05) <.001**	**-0.55(0.03) <.001**	**-0.26(0.04) <.001**	**-0.19(0.03) <.001**	**-0.18(0.03) <.001**	**-0.26(0.03) <.001**
	Thal 9p+bp+ss	Puta 9p+bp+ss	Cere 9p+bp+ss	Exec 9p+bp+ss	Sali 9p+bp+ss	DMN 9p+bp+ss
Int.	0.6(0.07)	0.69(0.06)	0.39(0.05)	0.45(0.05)	0.29(0.04)	0.49(0.05)
SB3.3	**0.45(0.09) <.001**	**0.28(0.08) <.001**	-0.04(0.04) 0.398	0.03(0.05) 0.541	0.1(0.04) 0.012	0.11(0.05) 0.027
MB 2	**0.18(0.07) 0.008**	0.06(0.07) 0.388	-0.05(0.05) 0.336	-0.09(0.05) 0.05	0.05(0.04) 0.282	0.03(0.05) 0.547
MB 3	0.16(0.08) 0.037	0.04(0.07) 0.538	-0.06(0.06) 0.345	-0.05(0.04) 0.238	0.02(0.05) 0.7	0(0.06) 0.987
MB 4	**0.34(0.08) <.001**	**0.17(0.06) 0.004**	0(0.04) 0.975	0.03(0.05) 0.569	0.08(0.04) 0.046	0.03(0.04) 0.448
MB 6	**0.3(0.06) <.001**	0.14(0.06) 0.012	-0.04(0.06) 0.456	-0.02(0.05) 0.725	0.07(0.03) 0.033	0.11(0.04) 0.011
MB 8	0.08(0.06) 0.179	0.09(0.05) 0.068	-0.11(0.04) 0.012	-0.04(0.04) 0.375	0.08(0.04) 0.026	**0.09(0.03) 0.006**
MB 9	0.04(0.08) 0.646	0(0.07) 0.981	-0.12(0.05) 0.016	-0.06(0.05) 0.178	0.03(0.04) 0.426	-0.02(0.06) 0.773
MB 12	0.05(0.06) 0.375	**-0.14(0.05) 0.008**	-0.1(0.06) 0.088	0(0.04) 0.936	-0.01(0.04) 0.843	-0.01(0.04) 0.71

Table S.1: Impact of MB factor on Fisher z-transformed correlations for selected edges in spatially smoothed data (6-mm FWHM). Estimates, standard errors, and p-values (uncorrected) from generalized estimating equations with robust standard errors. The intercept is the average Fisher z-transformed correlation for edges in the indicated community for SB 2 mm controlling for gender and scanner. P-values represent whether the correlation of the acquisition differs significantly from SB 2 mm. Differences with $p \leq 0.001$ are in bold and colored red for acquisitions significantly lower than 2 mm and blue for acquisitions significantly higher. Top: 9p+spatial smoothing. Bottom: 9p+bandpass+spatial smoothing.

	SB 3.3 mm	SB 2 mm	MB 2	MB 3
Auditory	0.005 p=0.765	**-0.042 p=0.008**	-0.041 p=0.022	-0.01 p=0.474
Cerebellum	-0.007 p=0.171	0.001 p=0.71	-0.002 p=0.55	-0.001 p=0.838
CO-Task Ctrl	0.001 p=0.966	**-0.051 p=0**	-0.039 p=0.048	-0.016 p=0.442
Default Mode	**-0.043 p=0.001**	**-0.059 p=0**	-0.033 p=0.016	-0.025 p=0.07
Dorsal Att	-0.014 p=0.048	**-0.023 p=0**	-0.01 p=0.066	-0.003 p=0.618
FP-Task Ctrl	-0.007 p=0.244	-0.005 p=0.234	-0.005 p=0.385	-0.002 p=0.748
Memory	-0.003 p=0.772	-0.011 p=0.364	-0.003 p=0.747	0.008 p=0.476
Salience	-0.014 p=0.067	**-0.025 p=0**	**-0.027 p=0**	-0.014 p=0.082
Som-Hand	0.011 p=0.513	0.005 p=0.793	-0.02 p=0.096	-0.004 p=0.74
Som-Mouth	0.009 p=0.684	-0.027 p=0.086	-0.027 p=0.082	0.009 p=0.619
Subcortical	0.023 p=0.097	-0.018 p=0.022	0.007 p=0.473	0.001 p=0.904
Ventral Att	0.01 p=0.384	-0.003 p=0.78	-0.005 p=0.589	-0.003 p=0.783
Visual	-0.023 p=0.012	**-0.039 p=0.002**	**-0.035 p=0.001**	-0.018 p=0.227
All	-0.014 p=0.053	**-0.029 p=0**	**-0.022 p=0.002**	-0.011 p=0.149
	MB 4	MB 6	MB 9	MB 12
Auditory	0.019 p=0.362	0.025 p=0.178	-0.029 p=0.072	**-0.075 p=0**
Cerebellum	0.008 p=0.159	0.003 p=0.728	0.007 p=0.324	-0.012 p=0.055
CO-Task Ctrl	0.023 p=0.381	0.008 p=0.708	-0.026 p=0.208	**-0.073 p=0.001**
Default Mode	-0.019 p=0.205	-0.007 p=0.584	**-0.03 p=0.008**	**-0.054 p=0**
Dorsal Att	0.004 p=0.535	-0.005 p=0.528	-0.013 p=0.036	**-0.024 p=0.004**
FP-Task Ctrl	0.011 p=0.062	0.017 p=0.012	0 p=0.94	-0.012 p=0.025
Memory	0.008 p=0.546	0.004 p=0.766	-0.014 p=0.118	-0.02 p=0.065
Salience	-0.003 p=0.724	0 p=0.972	-0.018 p=0.018	**-0.038 p=0**
Som-Hand	0.016 p=0.34	0.029 p=0.143	-0.013 p=0.297	-0.027 p=0.092
Som-Mouth	-0.017 p=0.258	0.019 p=0.406	0.007 p=0.665	-0.037 p=0.037
Subcortical	0.026 p=0.06	0.028 p=0.07	-0.009 p=0.41	**-0.051 p=0**
Ventral Att	0.026 p=0.039	0.013 p=0.337	-0.005 p=0.632	**-0.032 p=0.001**
Visual	-0.019 p=0.2	-0.008 p=0.479	-0.024 p=0.057	**-0.034 p=0.009**
All	0.001 p=0.952	0.006 p=0.458	**-0.018 p=0.004**	**-0.04 p=0**

Table S.2: Difference between the proportion of significant edges in the indicated acquisition versus MB 8 in 9p preprocessing, where negative values indicate greater activation in MB 8. Proportions for a given community include all edges in which at least one node belonged to the community. P-values are based on 10,000 permutations and are not corrected for multiple comparisons. Bold indicates $p < 0.01$.

	SB 3.3 mm	SB 2 mm	MB 2	MB 3
Auditory	0 p=0.995	**-0.054 p=0.007**	**-0.07 p=0.007**	-0.015 p=0.469
Cerebellum	-0.014 p=0.087	-0.004 p=0.674	-0.007 p=0.519	0 p=0.969
CO-Task Ctrl	-0.013 p=0.548	**-0.062 p=0.001**	-0.059 p=0.021	-0.017 p=0.46
Default Mode	**-0.062 p=0**	**-0.09 p=0**	-0.052 p=0.011	-0.036 p=0.066
Dorsal Att	**-0.024 p=0.008**	**-0.042 p=0**	**-0.031 p=0**	-0.013 p=0.135
FP-Task Ctrl	-0.01 p=0.267	**-0.018 p=0.009**	-0.016 p=0.079	-0.01 p=0.286
Memory	-0.014 p=0.385	-0.019 p=0.244	-0.016 p=0.293	0.005 p=0.728
Salience	-0.022 p=0.046	**-0.042 p=0**	**-0.052 p=0**	-0.018 p=0.144
Som-Hand	0.004 p=0.865	-0.004 p=0.862	-0.04 p=0.015	-0.011 p=0.533
Som-Mouth	0.015 p=0.622	-0.047 p=0.102	-0.051 p=0.012	0.014 p=0.634
Subcortical	0.002 p=0.876	**-0.049 p=0**	-0.018 p=0.123	-0.026 p=0.085
Ventral Att	0.009 p=0.571	-0.014 p=0.261	-0.01 p=0.41	0 p=0.97
Visual	-0.034 p=0.018	**-0.053 p=0.006**	**-0.048 p=0.003**	-0.024 p=0.247
All	**-0.024 p=0.01**	**-0.047 p=0**	**-0.04 p=0**	-0.019 p=0.082

	MB 4	MB 6	MB 9	MB 12
Auditory	0.004 p=0.881	0.021 p=0.274	-0.026 p=0.22	**-0.078 p=0.001**
Cerebellum	-0.003 p=0.753	0.005 p=0.849	0.001 p=0.914	-0.018 p=0.126
CO-Task Ctrl	0.006 p=0.784	-0.004 p=0.864	-0.023 p=0.342	**-0.069 p=0.003**
Default Mode	-0.033 p=0.098	-0.018 p=0.324	**-0.048 p=0.004**	**-0.068 p=0**
Dorsal Att	-0.015 p=0.096	-0.01 p=0.375	-0.01 p=0.16	-0.022 p=0.067
FP-Task Ctrl	0.001 p=0.89	0.011 p=0.227	-0.004 p=0.66	-0.022 p=0.01
Memory	-0.002 p=0.923	0.009 p=0.667	-0.022 p=0.166	-0.002 p=0.855
Salience	-0.003 p=0.853	-0.005 p=0.75	-0.011 p=0.302	**-0.051 p=0**
Som-Hand	0.008 p=0.738	0.017 p=0.476	-0.012 p=0.518	-0.036 p=0.077
Som-Mouth	-0.034 p=0.122	0.005 p=0.833	0.015 p=0.591	-0.045 p=0.098
Subcortical	0.015 p=0.387	0.011 p=0.46	-0.01 p=0.508	**-0.084 p=0**
Ventral Att	0.031 p=0.03	0.01 p=0.534	-0.001 p=0.924	**-0.042 p=0.004**
Visual	-0.03 p=0.189	-0.009 p=0.593	-0.03 p=0.139	-0.046 p=0.01
All	-0.01 p=0.466	-0.001 p=0.919	-0.022 p=0.032	**-0.049 p=0**

Table S.3: Difference between the proportion of significant correlations in the indicated acquisition versus MB 8 in 9p+spatial smoothing preprocessing, where negative values indicate greater activation in MB 8. Proportions for a given community include all edges in which at least one node belonged to the community. P-values are based on 10,000 permutations and are not corrected for multiple comparisons. Results are similar to those from the unsmoothed data in Table S.2. Bold indicates $p < 0.01$.

	SB 3.3 mm	SB 2 mm	MB 2	MB 3
Auditory	-0.001 p=0.934	-0.051 p=0.011	**-0.059 p=0**	-0.026 p=0.108
Cerebellum	-0.002 p=0.546	0.004 p=0.291	-0.002 p=0.625	0.002 p=0.625
CO-Task Ctrl	-0.008 p=0.681	**-0.056 p=0.001**	-0.051 p=0.021	-0.018 p=0.387
Default Mode	**-0.038 p=0.006**	**-0.052 p=0**	-0.035 p=0.026	-0.026 p=0.051
Dorsal Att	-0.015 p=0.018	**-0.019 p=0.001**	-0.012 p=0.074	-0.003 p=0.671
FP-Task Ctrl	-0.003 p=0.597	0.004 p=0.347	0.001 p=0.806	0.008 p=0.089
Memory	-0.004 p=0.663	-0.008 p=0.468	-0.011 p=0.275	0.008 p=0.408
Salience	-0.008 p=0.233	-0.017 p=0.02	-0.02 p=0.017	-0.009 p=0.279
Som-Hand	0.008 p=0.65	0.001 p=0.935	**-0.028 p=0.002**	-0.012 p=0.338
Som-Mouth	0.011 p=0.662	-0.021 p=0.272	**-0.032 p=0.003**	-0.015 p=0.347
Subcortical	0.004 p=0.671	**-0.023 p=0.002**	-0.001 p=0.923	-0.008 p=0.348
Ventral Att	0.01 p=0.364	-0.001 p=0.849	0 p=0.918	0.004 p=0.67
Visual	-0.015 p=0.168	-0.025 p=0.088	-0.025 p=0.035	-0.011 p=0.435
All	-0.012 p=0.076	**-0.025 p=0.001**	**-0.023 p=0.002**	-0.012 p=0.098
	MB 4	MB 6	MB 9	MB 12
Auditory	-0.027 p=0.112	0 p=0.996	-0.036 p=0.049	**-0.068 p=0**
Cerebellum	0.002 p=0.694	0.014 p=0.159	-0.008 p=0.184	-0.012 p=0.05
CO-Task Ctrl	-0.008 p=0.782	-0.014 p=0.587	-0.039 p=0.033	**-0.071 p=0.001**
Default Mode	-0.023 p=0.092	-0.017 p=0.309	-0.036 p=0.01	**-0.049 p=0.002**
Dorsal Att	-0.005 p=0.486	-0.007 p=0.267	-0.013 p=0.02	-0.015 p=0.013
FP-Task Ctrl	0.013 p=0.023	**0.017 p=0.004**	0.001 p=0.836	-0.002 p=0.702
Memory	0.002 p=0.881	0 p=0.982	-0.008 p=0.28	-0.016 p=0.138
Salience	0 p=0.956	-0.001 p=0.906	-0.018 p=0.015	-0.02 p=0.033
Som-Hand	0.003 p=0.852	0.018 p=0.382	-0.015 p=0.297	-0.018 p=0.178
Som-Mouth	-0.02 p=0.139	0.017 p=0.506	-0.003 p=0.828	-0.037 p=0.04
Subcortical	0.011 p=0.303	0.006 p=0.601	-0.005 p=0.526	**-0.033 p=0**
Ventral Att	0.016 p=0.141	0.004 p=0.708	-0.004 p=0.652	-0.02 p=0.049
Visual	-0.008 p=0.603	-0.009 p=0.479	-0.019 p=0.102	-0.024 p=0.087
All	-0.006 p=0.493	-0.001 p=0.915	**-0.02 p=0.003**	**-0.031 p=0**

Table S.4: Difference between the proportion of significant correlations in the indicated acquisition versus MB 8 in 9p+bandpass preprocessing, where negative values indicate greater activation in MB 8. Proportions for a given community include all edges in which at least one node belonged to the community. P-values are based on 10,000 permutations and are not corrected for multiple comparisons. Bold indicates $p < 0.01$.

	SB 3.3 mm	SB 2 mm	MB 2	MB 3	MB 4
Auditory	0.019 p=0.02	**0.013 p=0.008**	**0.021 p=0.002**	0.019 p=0.017	**0.051 p=0**
Cerebellum	-0.001 p=0.62	0 p=0.861	0.003 p=0.218	0.002 p=0.526	**0.009 p=0.008**
CO-Task Ctrl	**0.021 p=0.002**	0.013 p=0.023	**0.023 p=0.008**	0.018 p=0.023	**0.047 p=0.003**
Default Mode	0.009 p=0.069	0.008 p=0.022	**0.016 p=0.006**	0.014 p=0.031	**0.021 p=0.002**
Dorsal Att	**0.01 p=0**	0.005 p=0.017	0.007 p=0.063	0.008 p=0.064	**0.017 p=0**
FP-Task Ctrl	**0.01 p=0.001**	0.007 p=0.017	0.008 p=0.021	0.006 p=0.041	**0.01 p=0.003**
Memory	0.009 p=0.033	0.004 p=0.194	0.01 p=0.02	-0.001 p=0.897	0.009 p=0.292
Salience	**0.013 p=0.008**	**0.011 p=0.001**	**0.013 p=0**	**0.015 p=0.003**	**0.02 p=0.001**
Som-Hand	0.008 p=0.141	0.011 p=0.014	0.009 p=0.047	**0.014 p=0.002**	0.019 p=0.042
Som-Mouth	0.009 p=0.328	0.005 p=0.259	0.012 p=0.043	**0.033 p=0**	0.013 p=0.035
Subcortical	**0.029 p=0**	**0.018 p=0**	**0.017 p=0**	**0.016 p=0.001**	**0.033 p=0**
Ventral Att	**0.018 p=0.001**	**0.019 p=0**	0.012 p=0.04	**0.015 p=0.004**	**0.031 p=0**
Visual	**0.013 p=0.006**	**0.009 p=0.004**	**0.013 p=0.002**	**0.015 p=0.004**	0.01 p=0.078
All	**0.012 p=0**	**0.009 p=0**	**0.013 p=0**	**0.013 p=0**	**0.021 p=0**

	MB 6	MB 8	MB 9	MB 12
Auditory	**0.031 p=0.002**	0.006 p=0.691	0.019 p=0.05	-0.001 p=0.893
Cerebellum	-0.008 p=0.158	0.003 p=0.517	0.013 p=0.012	0.003 p=0.298
CO-Task Ctrl	**0.033 p=0.001**	0.01 p=0.58	0.019 p=0.19	0.008 p=0.517
Default Mode	**0.02 p=0.002**	0.011 p=0.282	0.015 p=0.015	0.006 p=0.322
Dorsal Att	**0.012 p=0.002**	0.01 p=0.046	0.009 p=0.079	0.001 p=0.672
FP-Task Ctrl	0.012 p=0.017	**0.012 p=0.007**	**0.011 p=0.009**	0.003 p=0.427
Memory	0.011 p=0.199	0.007 p=0.356	0.005 p=0.337	0.003 p=0.667
Salience	**0.02 p=0**	**0.019 p=0**	**0.018 p=0**	0.001 p=0.792
Som-Hand	0.017 p=0.039	0.006 p=0.547	0.013 p=0.072	-0.002 p=0.811
Som-Mouth	0.009 p=0.427	0.008 p=0.52	**0.033 p=0.002**	0.007 p=0.371
Subcortical	**0.034 p=0**	0.012 p=0.09	0.011 p=0.063	-0.006 p=0.103
Ventral Att	**0.028 p=0**	**0.019 p=0.001**	**0.017 p=0**	0.007 p=0.186
Visual	**0.019 p=0.001**	**0.019 p=0.009**	**0.015 p=0.007**	0.009 p=0.158
All	**0.019 p=0**	0.013 p=0.019	**0.014 p=0**	0.004 p=0.263

Table S.5: Difference in proportion of significant correlations between 9p and 9p+bandpass. Positive values indicate a higher proportion in 9p. Proportions for a given community include all edges in which at least one node belonged to the community. P-values are based on 10,000 permutations and are not corrected for multiple comparisons. Bold indicates $p < 0.01$. Overall, there are more significant edges in 9p. Bold indicates $p < 0.01$.
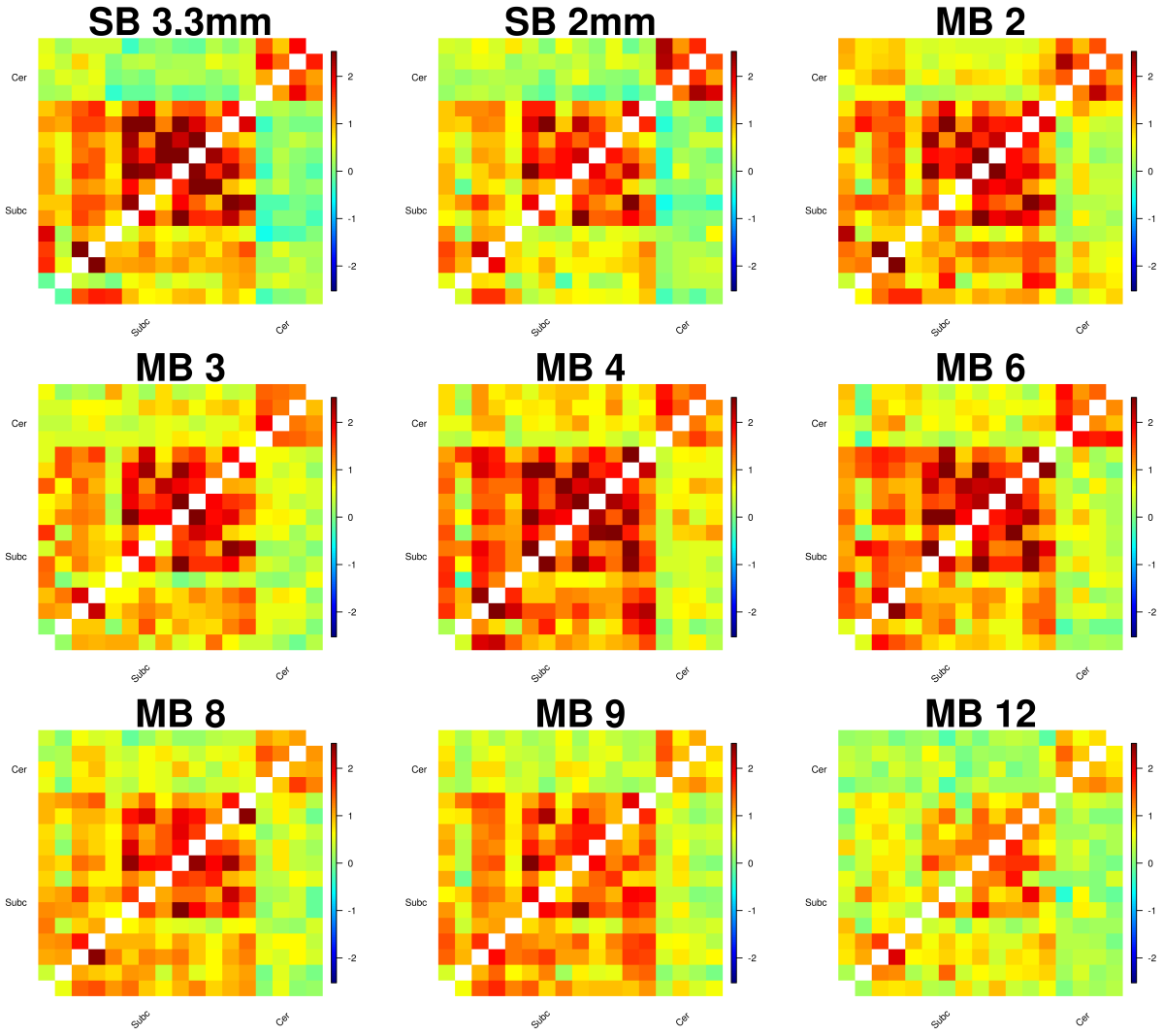
Figure S.11: Cohen's d for SB and MB acquisitions in subcortical and cerebellar regions. Cohen's d for preprocessing without bandpass filtering are above the diagonal, and those for bandpass filtering are below the diagonal.

S.4. Supplemental Materials for Validation on independent datasets

*S.4.1. Evaluation on a third scanner using a 64-channel head coil*
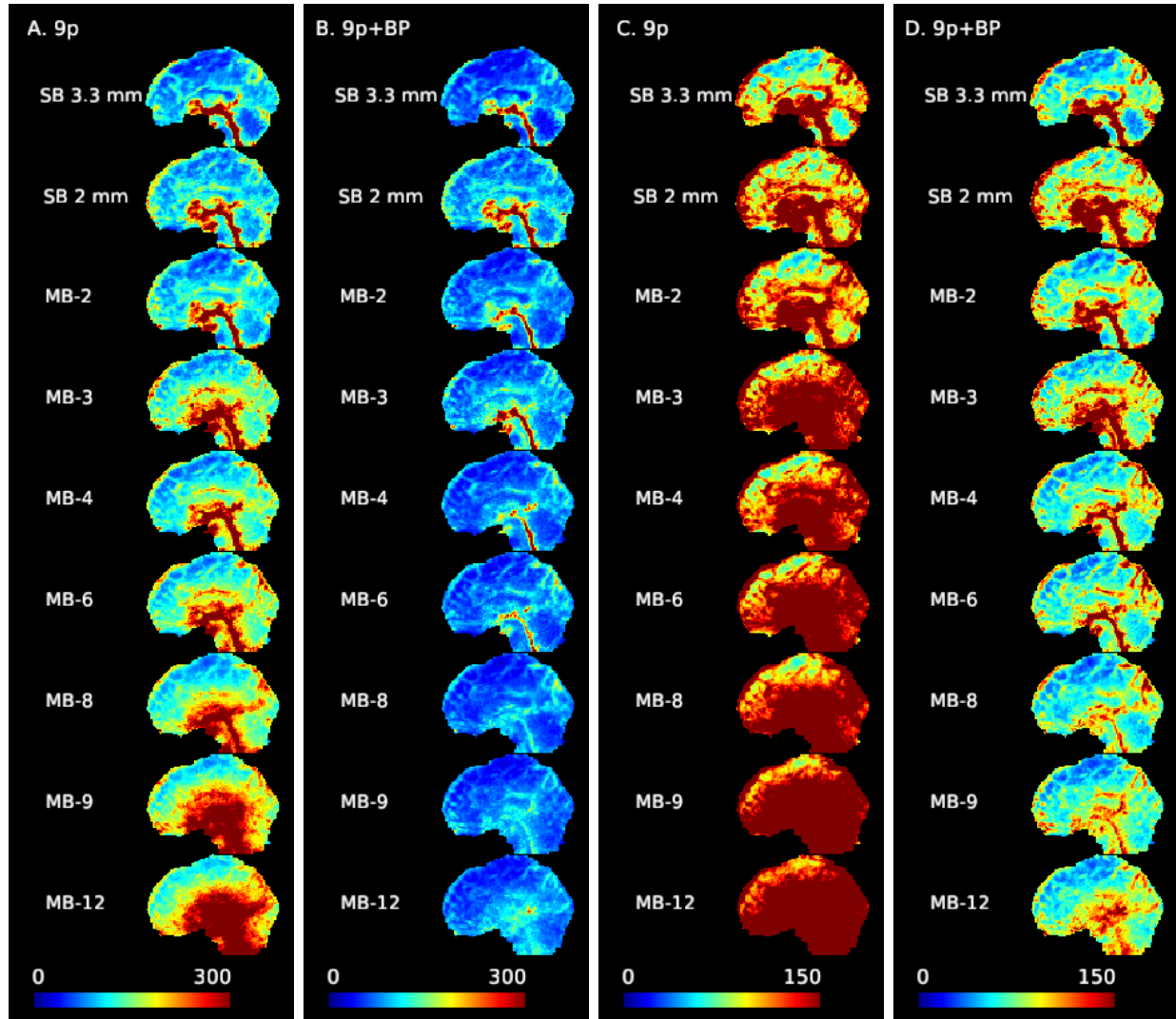
Figure S.12: Noise amplification due to multiband acceleration and impacts of bandpass filtering in the University of Rochester cohort (three subjects) using a 64-channel head coil. The standard deviation of the time series for each voxel averaged across the three subjects with 9p preprocessing (columns 1 and 3) and 9p+bandpass (columns 2 and 4). Sagittal slice with cursor at MNI=0. At higher MB factors, variance from noise amplification becomes more prominent. Columns 1 and 2 use a scale from 0 to 300, and columns 3 and 4 are the same data but using a scale from 0 to 150. The results appear similar to the thirty-two subjects on the 32-channel head coil.
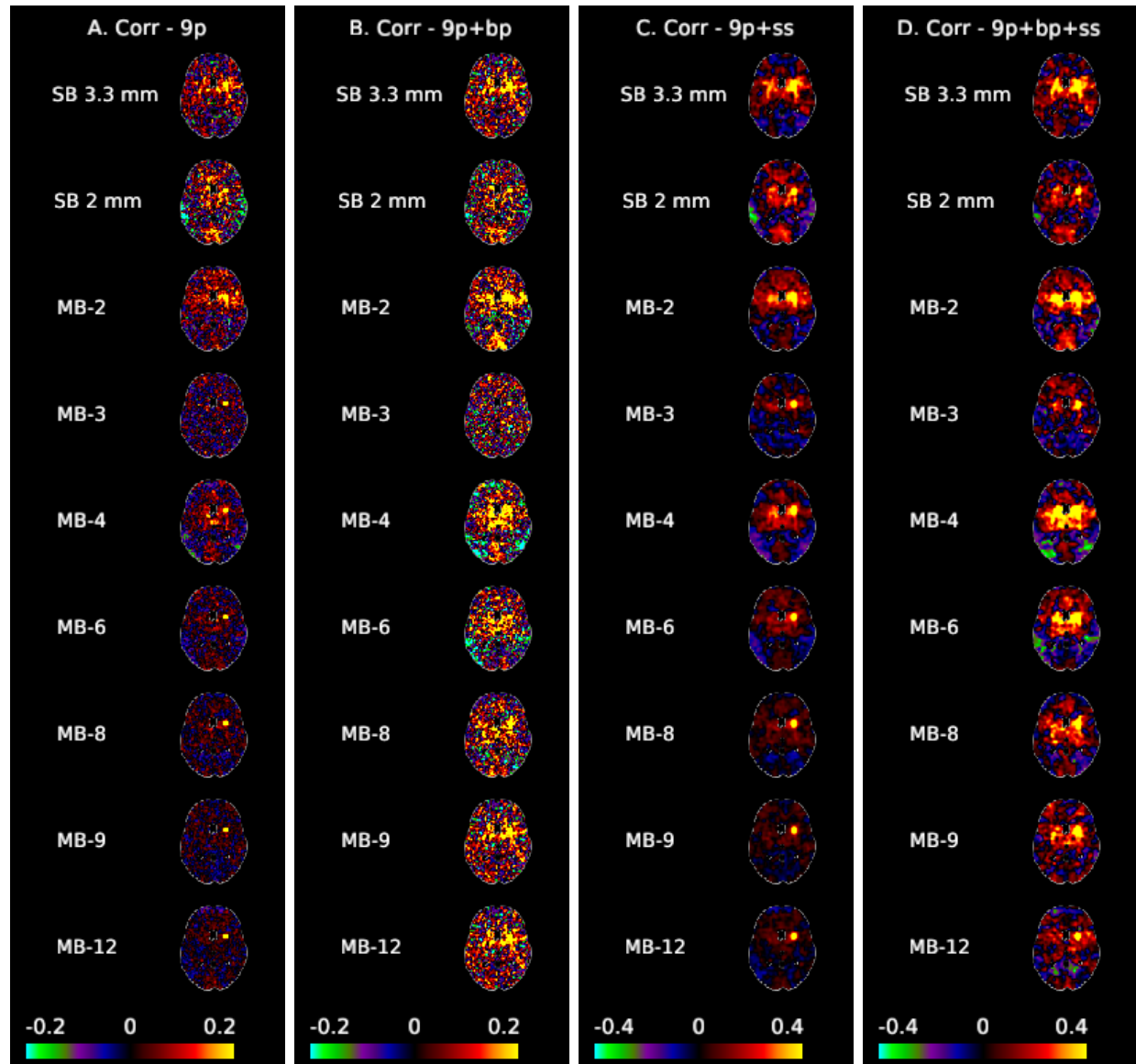
Figure S.13: Correlations averaged across the three subjects from the University of Rochester cohort with 9p (A), 9p+bandpass (B), 9p+spatial smoothing (C), and 9p+bandpass+spatial smoothing (D) for the dorsal rostral putamen seed (MNI: 25, 8, 6) shown at MNI axial slice 6. The unsmoothed data show high variability (A and B). In 9p+spatial smoothing (C), a similar pattern as in the Emory cohort is observed, with spatial biases increasing as MB factor increases. These biases are reduced with bandpass filtering (D), which generally results in greater correlations with the left putamen.
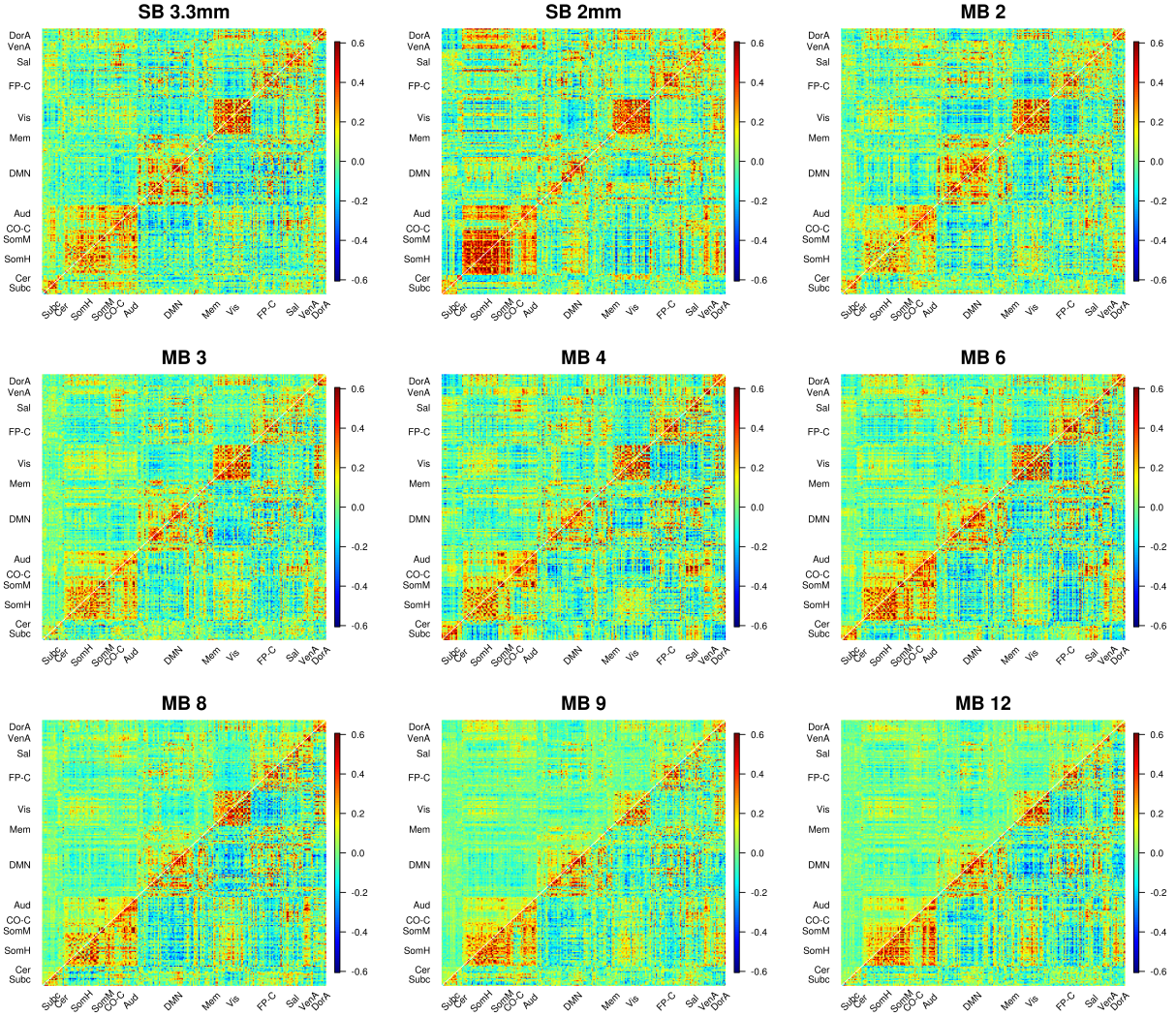
Figure S.14: Average correlations (Fisher z-transformed) for SB and MB acquisitions in the three subjects from the University of Rochester cohort. 9p processing is above the diagonal and 9p+bandpass below. In 9p, correlations tend to be similar within the visual system for SB through MB 8; subcortical correlations tend to be smaller in MB 8, MB 9, and MB 12 than SB 3.3, MB 2, MB 4, and MB 6 (above diagonal). In 9p+BP, temporal filtering again tends to make the magnitudes of correlations more comparable across acquisitions (below diagonal). SB 2 mm appears to have very strong cortical connectivity, which appears to be the result of high connectivity in one of the three subjects. This subject exhibited comparatively high connectivity in their SB 2 mm scan but not their other scans.

S.4.2. Evaluation of pairwise correlations in the preprocessed Young Adult Human Connec-
tome Project data

The HCP used MB 8 collected on a customized Siemens Skyra 3T and contains 4 15-min 2-mm isotropic rs-fMRI scans from 1003 subjects (2 scans have left-right phase encoding, 2 scans have right-left phase encoding). We used the data in "cifti" format (vertices for the cortical surface plus voxels for the subcortical and cerebellum regions), specifically,

`<subjectID>_rfMRI_REST1_LR_Atlas_MSMAll_hp2000_clean.dtseries.nii`.

The ICA-FIX preprocessing performs targeted removal of motion and physiological artifacts, where the time courses of independent components identified as artifacts are regressed out of the data. Also note that this pipeline does not include global signal regression. See Smith et al. (2013) for details.

For each scan, the time series of each vertex/voxel was centered and standardized to unit variance. We then calculated the time series for each region by averaging vertices within regions defined by the multi-modal parcellation (360 regions) (Glasser et al., 2016) and the nineteen non-cortical gray matter regions, resulting in 379 time series for each scan. The correlations were then calculated and Fisher-transformed for each scan, and then the four scans were averaged for each subject. We then averaged the 1003 correlation matrices to create the group average correlation matrix. We also calculated the standard deviation (across the 1003 subjects) for each edge. We then calculated a Cohen's d matrix from the group average matrix divided by the standard deviations. Cortical areas were grouped into functional communities using Akiki and Abdallah (2018).

If functional connectivity between regions is apparent in the Cohen's d matrix, but less apparent in the correlation matrix, we view this as additional evidence that Cohen's d maps can aid in quantifying functional connectivity in MB acquisitions.

We see that many subcortical to subcortical and subcortical to cortical correlations appear weak in the correlation matrix. In contrast, functional connectivity between these regions is more prominent in the Cohen's d matrix (Figure S.15). For example, the correlations between subcortical and central executive nodes are generally small in the correlations, while they have large Cohen's d. This suggests that lower correlations in many subcortical regions is a general feature of multiband acquisitions, and that Cohen's d can aid in the adjudication of functional connectivity in these regions.

We note that a drawback of this parcellation is that the standard deviation may be reduced in large regions, as the signal is averaged over more locations. For example, the standard deviation in the cerebellum may be much smaller than the standard deviation in a small cortical region. On the other hand, there may be a loss in the strengths of correlations, as specificity is reduced by averaging over large regions. Also note that since we use the average correlation from four 15-min scans for each subject, the standard deviation used in the Cohen's d calculation is reduced relative to a single 6-min scan, resulting in larger effects sizes than the Emory cohort.
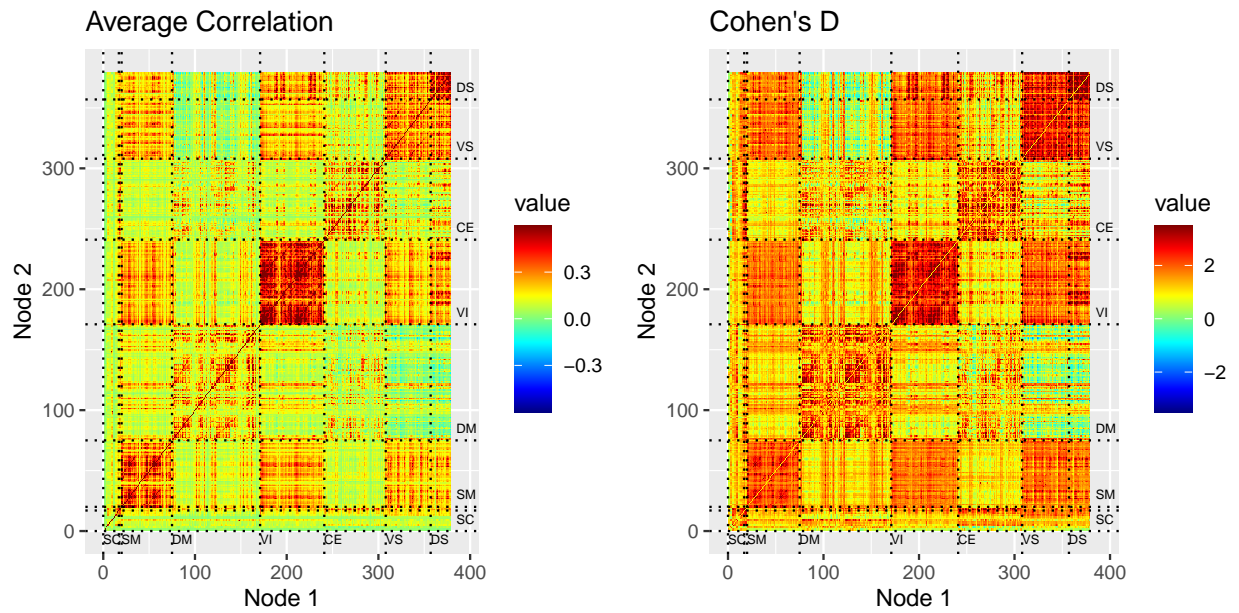
Figure S.15: The correlation matrix between nodes of the multimodal parcellation augmented with nineteen gray matter structures (left) and Cohen's d (right). SC=subcortical, which is followed by the brainstem and left and right cerebellum (unlabeled), SM=somatomotor, DM=default mode, VI=visual, CE=central executive, VS=ventral salience, DS=dorsal salience. Communities defined using Akiki and Abdallah (2018). In the average correlation matrix, most subcortical edges show small correlations, suggesting weak or no functional connectivity. In the Cohen's d matrix, the effect sizes indicate functional connectivity between many subcortical and cortical regions.

References

Akiki, T. J. and Abdallah, C. G. (2018). Determining the Hierarchical Architecture of the Human Brain Using Subject-Level Clustering of Functional Networks. *bioRxiv*, page 350462.

Buckner, R. L., Krienen, F. M., Castellanos, A., Diaz, J. C., and Thomas Yeo, B. T. (2011). The organization of the human cerebellum estimated by intrinsic functional connectivity. *Journal of Neurophysiology*, 106(5):2322–2345.

Glasser, M. F., Coalson, T. S., Robinson, E. C., Hacker, C. D., Harwell, J., Yacoub, E., Ugurbil, K., Andersson, J., Beckmann, C. F., Jenkinson, M., and others (2016). A multimodal parcellation of human cerebral cortex. *Nature*, 536(7615):171–178.

Smith, S. M., Beckmann, C. F., Andersson, J., Auerbach, E. J., Bijsterbosch, J., Douaud, G., Duff, E., Feinberg, D. A., Griffanti, L., Harms, M. P., and others (2013). Resting-state fMRI in the human connectome project. *Neuroimage*, 80:144–168.